iJRASET
International Journal For Research in Applied Science and Engineering Technology

INTERNATIONAL JOURNAL FOR RESEARCH

IN APPLIED SCIENCE & ENGINEERING TECHNOLOGY

Volume: 3 **Issue:** III **Month of publication:** March 2015

DOI:

www.ijraset.com

Call: 08813907089 | E-mail ID: ijraset@gmail.com

International Journal for Research in Applied Science & Engineering Technology (IJRASET)

Micro converter fed BLDC motor using PV applications

Yogaprasad R[1], Thangarasu S[2], N.Prakash[3]

Abstract-In this paper using a transformer less step up voltage method is used. Reduced the losses and improved the power quality by using this proposed method. Within the photovoltaic (PV) power-generation marketplace, the ac PV module has shown clear growth. However, a high voltage gain converter is necessary for the module's grid connection through a direct current –alternate current inverter. In this proposes a converter that employs a suspended active switch to isolate energy from the PV panel when the ac module is OFF; this exacting design protects installers and users from electrical hazards. Without excessive duty ratios and the frequent turns-ratios of a coupled inductor, this converter achieves a step-up voltage-conversion ratio; the leakage inductor energy of the coupled inductor is efficiently to the load. These features explain the module's high-efficiency performance. The full operating principles continuous, discontinuous, and boundary conduction modes are describe. A 15V input voltage, 300V output voltage model circuit of the proposed converter has been implemented; its maximum efficiency is up to 95.3% and full-load efficiency is 92.3%.

Index Terms—PV module, coupled inductor, step-up voltage, single switch, BLDC motor.

I. INTRODUCTION

Photovoltaic (pv) power-generation systems are becoming increasingly important and prevalent in distribution generation systems. A conservative national PV array is a serial connection of numerous panels to obtain higher dc-link voltage for main electricity through a dc–ac inverter [1], [13]. Unfortunately, once there is a partial shadow on some panels, the system's energy yield becomes considerably reduced [2]. An ac module is a micro inverter configured on the rear bezel of a PV panel [1]–[3]; this alternative solution not only immunizes against the yield loss by shadow effect, but also provides bendable installation options in accordance with the user's budget [4]. Many prior research works have proposed a single-stage dc–ac inverter with fewer components to fit the dimensions of the bezel of the ac part, but their efficiency levels are lower than those of conventional PV inverters. The power capacity range of a single PV panel is about 100W to 300W, and the maximum power point (MPP) voltage range is from 15V to 28V, which will be the input voltage of the ac module; in cases with lower input voltage, it is difficult for the ac module to reach

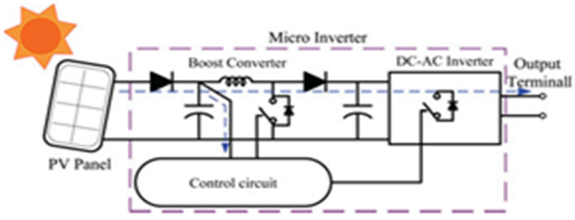

Figure .1.Circuit diagram of micro converter.

efficiency [3]. Employing a high step-up dc–dc converter in the front of the inverter improves power-conversion at high efficiency and provides a constant dc link to the inverter.

Installing the PV generation system during sunshine, for safety reasons, the ac module outputs zero voltage [4], [5]. Fig. 1 shows the solar energy through the PV panel and this inverter to the output terminal when the switches are OFF. When mechanism of the ac module is taking place, this potential difference could create hazards to both the worker and the conveniences. A balanced active switch is designed to isolate the dc current from the PV board, for when the ac module is off-grid as fit as in the non operating

condition. This isolation ensures the method of the internal components without any residential energy being transferred to the output or input terminals, which could be dangerous. The micro inverter includes dc–dc boost converter, dc–ac conversion with control circuit as shown in Fig. 1. The dc–dc converter requires large step-up conversion from the board's low voltage to the voltage level of the application. Earlier research on various converters for high step-up applications has integrated analyses of the switched-inductor and switched-capacitor types [6], [7]; transformer less switched-capacitor type [8], [9], the voltage-lift type [12]; the capacitor-diode voltage product [13]; and the increase type integrated with a coupled inductor [10], [11], these converters by rising turns ratio of coupled inductor obtain voltage gain than conventional increase converter. Some converters effectively combined boost and flyback converters, while various converter combinations are developed to take out high step-up voltage gain by using the coupled-inductor technique. The effectiveness and voltage gain of the dc–dc boost converter are forced by either the freeloading effect of the power switches or the reverse recovery issue of the diodes. In adding, the equivalent series resistance (ESR) of the capacitor and the parasitic resistances of the inductor also affect overall efficiency. Active clamp technique not only reuses the leakage inductor's energy but also constrains the voltage oscillation across the active switch, though the exchange is higher cost and difficult control circuit [17], [18]. Combining active snubber, auxiliary resonant circuit, rectifiers, or switched- capacitor-based resonant circuits and so on, these techniques ready active switch into zero voltage switching (ZVS) or zero current switching (ZCS) operation and improved efficiency .The leakage-inductor energy from the coupled inductor can be reused, the voltage oscillation on the active switch is decreased, which means the coupled inductor employed in mixture with the voltage-multiplier or voltage-lift technique effectively accomplishes the aim of higher voltage gain [6]–[13].

The proposed converter, shown in Fig. 2, is comprised of a coupled inductor *T*1 with the balanced active switch *S*1. The main winding *N*1 of a coupled inductor *T*1 is like to the input inductor of the conventional boost converter, and capacitor *C*1 and diode *D*1 get leakage inductor energy from *N*1 and the secondary winding *N*2 of coupled inductor *T*1 is connected with another pair of capacitors *C*2 and diode *D*2 are in series with *N*1 in order to add the voltage. The rectifier diode *D*3 connects to its output capacitor *C*3.

The proposed converter has more than a few features:

A. The connection of the two pairs of inductors, capacitor, and diode gives a large step-up voltage-conversion percentage;
B. The leakage-inductor energy of the coupled inductor can be reuse, thus increasing the efficiency and restraining the voltage oscillation across the active switch; and
C. The balanced active switch efficiently isolates the PV panel energy during non operating setting, which enhances shelter. The operating principles of the proposed converter are presented in the following sections.

II. OPERATING PRINCIPLES OF THE MICRO CONVERTER

The simplified circuit model of the proposed converter is shown in Fig. 3. The coupled inductor *T*1 is represented as a magnetizing inductor *Lm*, primary and secondary leakage inductors *Lk* 1 and *Lk* 2, and an ideal transformer. In order to simplify the circuit analysis of the proposed converter, the following assumptions are made.

A. All components are ideal, except for the leakage inductance of coupled inductor *T*1, which is being taken under consideration the on-state resistance *R*DS (ON) and all parasitic capacitances of the main switch *S*1 are neglected, as are the forward voltage drops of diodes *D*1, *D*3.
B. The capacitors *C*1, *C*3 are sufficiently large that the voltages across them are considered to be constant.
C. The ESR of capacitors *C*1, *C*3 and the parasitic resistance of coupled inductor *T*1 are neglected.
D. The turn's ratio *n* of the coupled inductor *T*1 windings is equal to *N*2 /*N*1.

The operating principle of continuous conduction mode (CCM) is presented in detail. The current waveforms of major components are given in Fig. 6. There are five operating modes in a switching period. The operating modes are described as follows.

Volume 3 Issue III, March 2015
ISSN: 2321-9653
International Journal for Research in Applied Science & Engineering Technology (IJRASET)

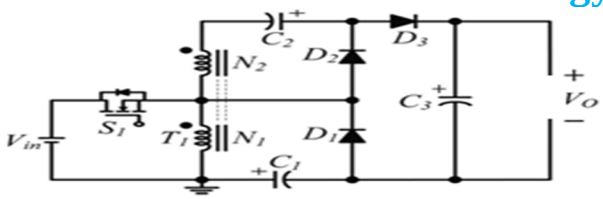

Fig. 2. Circuit configuration of proposed converter.

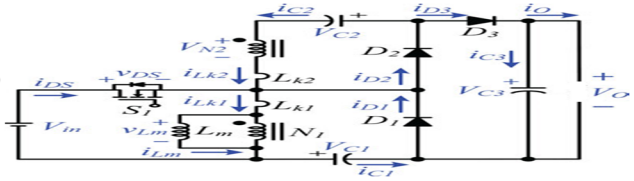

Fig. 3. Polarity definitions of voltage and current in proposed converter.

A. CCM Operation

1) *Mode I [t0, t1]:* In this alteration interval, the magnetizing inductor *Lm* incessantly charges capacitor *C*2 through *T*1 when *S*1 is turned ON. The current flow pathway is shown in Fig. 4(a); switch *S*1 and diode *D*2 are conduct. The current *iLm* is falling because source voltage *V*in crosses magnetizing inductor *Lm* and primary leakage inductor *Lk*1; magnetizing inductor *Lm* is transferring its energy through coupled inductor *T*1 to charge switched capacitor *C*2 , but the energy is falling; the charging current *iD* 2 and *iC*2 are falling. The secondary leakage inductor current *iLK*2 is equal to *iLm* / *n*. Increasing *iLk*1 equals decreasing *iLm* at *t* = *t*1, this mode ends.
2) *Mode II [t1, t2]:* In this mode, source energy *V*in is series linked with *N*2 , *C*1 , and *C*2 to charge output capacitor *C*3 and load; magnetizing inductor *Lm* is also getting energy from *V*in . The current flow pathway is shown in Fig. 4(b), where switch *S*1 remains ON, and diode *D*3 is conducting. The *iLm*, *iLk*1 , and *iD*3 are rising because the *V*in is crossing *Lk*1 , *Lm*, and primary winding *N*1 ; *Lm* and *Lk*1 are store energy from *V*in ; mean *V*in is also serially connected with secondary winding *N*2 of coupled inductor*T*1 , capacitors *C*1 , and *C*2 , and after that discharges their energy to capacitor *C*3 and load. The *i*in , *iD* 3 and discharge current |*iC*1 | and |*iC*2 | are rising. This mode ends while switch *S*1 is turned OFF at *t* = *t*2.
3) *Mode III [t2, t3]:*In this interval, secondary leakage inductor *Lk*2 keeps charging *C*3 while switch *S*1 is OFF. The current flow pathway is shown in Fig. 4(c), where only diode *D*1 and *D*3 are conduct. The energy stored in leakage inductor *Lk*1 flows through diode *D*1 to capacitor *C*1 immediately when *S*1 is OFF. While, the energy of secondary leakage inductor *Lk*2 is series connected with *C*2 to charge output capacitor *C*3 and the load. Leakage inductance *Lk*1 and*LK*2 are smaller than *Lm*, *iLk*2 quickly decreases, but *iLm* is rising because magnetizing inductor *Lm* is getting energy from *Lk*1. Current *iLk*2 reduced until it reaches zero; this mode ends at *t* = *t*3.
4) *Mode IV [t3, t4]:* In this interval, the energy stored in magnetizing inductor *Lm* is delivered to *C*1 and *C*2 concurrently. The current flow pathway is shown in Fig. 4(d). Only diodes *D*1 and *D*2 are conducting. Currents *iLk*1 and *iD*1 are

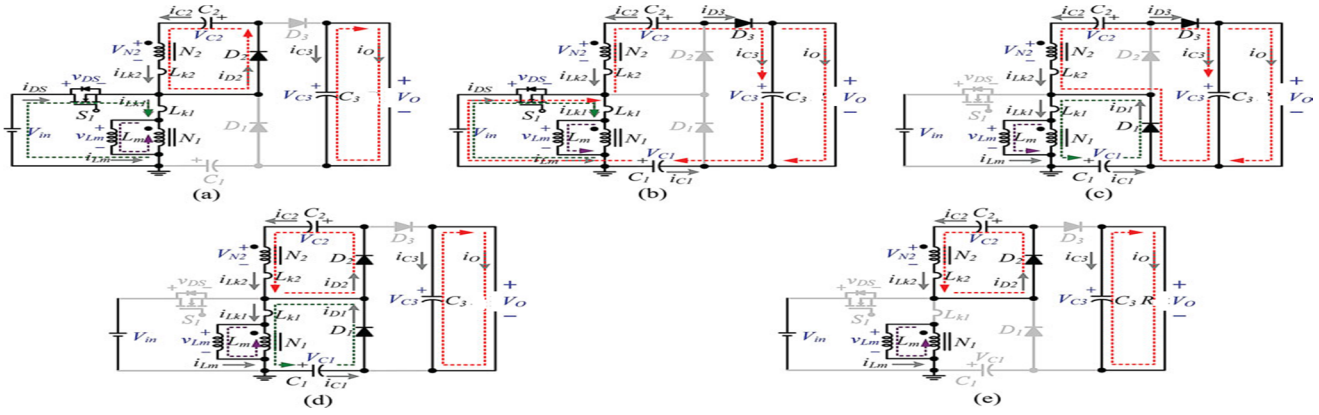

Fig.4. Current flow path of five operating modes during one switching period at CCM operation. (a) Mode I: *t*0 , *t*1 . (b) Mode II: *t*1 ,*t*2 . (c) Mode III: *t*2 ,*t*3 . (d) Mode IV: *t*3, *t*4 . (e) Mode V: *t*4 , *t*5 .

Continually decreased because the leakage energy through diode*D*1 keeps charging capacitor *C*1. The *Lm* is delivering its energy through *T*1 and *D*2 to charge capacitor *C*2. The energy stored in capacitor *C*3 is always decreased to the load. These energy transfers result in decreases in *iLk*1and *iLm* but increases in *iLk*2. This mode ends when current *iLk*1 is zero, at *t* = *t*4.

5) *Mode V [t*4, *t*5]*:* During this interval, only magnetizing inductor *Lm* is constantly releasing its energy to *C*2 . The current flow pathway is shown in Fig. 4(e), in which only diode *D*2 is conducting. The *iLm* is falling due to the magnetizing inductor energy flow through the coupled inductor *T*1 to secondary winding *N*2 , and *D*2 continues to charge capacitor *C*2 . The energy stored in capacitor *C*3 is continually discharged to the load *R*. This mode ends when switch *S*1 is turned ON at the create of the next switching period.

B. DCM Operation

The full operating principles for is continuous conduction- mode (DCM) operation are existing in this section. Fig. 5 depicts several typical waveforms during five operating modes of one switching period. The operating modes are described as follows.

1) *Mode I [t*0, *t*1]*:* In this interval, source energy *V*in is series linked with *N*2 , *C*1 , and *C*2 to charge output capacitor *C*3 and load; magnetizing inductor *Lm* is also receiving energy from *V*in . The current flow pathway is shown in Fig. 5(a), it depicts that switch *S*1 remains ON, and only diode *D*3 is conducting. The *iLm*, *iLk*1 , and *iD*3 are rising because the *V*in is passage *Lk*1 , *Lm*, and primary winding *N*1 ; *Lm* and *Lk*1 are storing energy from *V*in ; *V*in also is serially linked with secondary winding *N*2 of coupled inductor *T*1 , capacitors *C*1 , and *C*2 ; then they all delivers their energy to capacitor *C*3 and load. The *i*in , *iD* 3 and delivers current |*iC*1 | and |*iC*2 | are rising. This mode ends when switch *S*1 is turned OFF at *t* = *t*1.

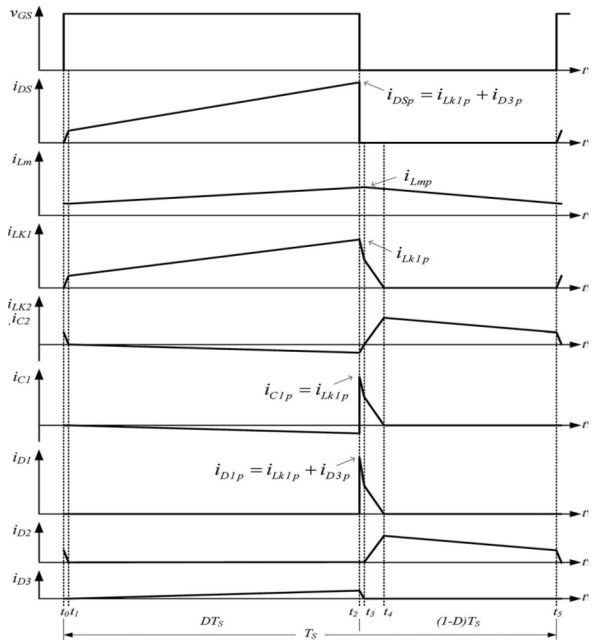

Fig. 5. Some typical waveforms of proposed converters at DCM operation.

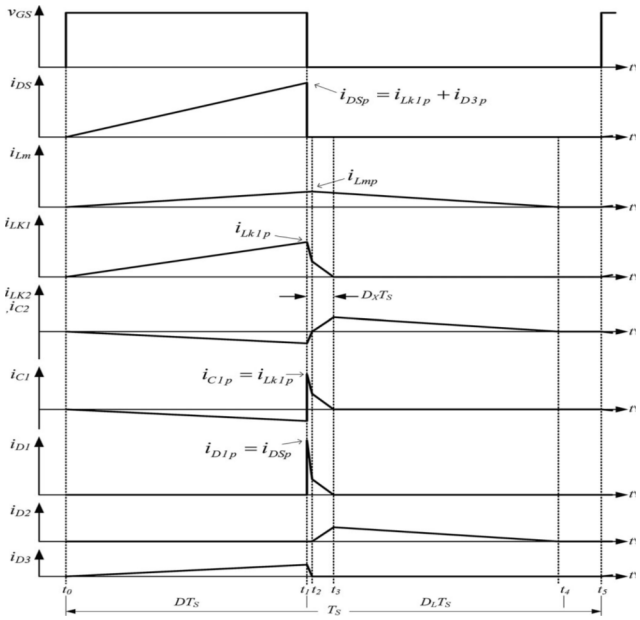

Fig. 6. Some typical waveforms of proposed converters at CCM operation.

2) *Mode II [t1, t2]:* In this mode, secondary leakage inductor *Lk*2 keeps charging *C*3 while switch *S*1 is OFF. The current pathway is shown in Fig. 4(b), and diode *D*2 and *D*3 are conducting. The energy stored in leakage inductor *Lk*1 through diode *D*1 to charge capacitor *C*1 instantly when *S*1 is OFF. Meanwhile, the energy of secondary leakage inductor *Lk*2 is series-connected with *C*2 to charge output capacitor *C*3 and the load. Because leakage inductance *Lk*1 and *LK*2 are smaller than *Lm*, *iLk*2 reduced rapidly, but *iLm* is rising because magnetizing inductor *Lm* is getting energy from *Lk*1. Current *iLk*2 get down to zero, and this mode ends at $t = t2$.
3) *Mode III [t2, t3]:* In this transition interval, the energy stored in coupled inductor *T*1 is delivere to *C*1 and *C*2. The current pathway is shown in Fig. 4(c). Diodes *D*1 and *D*2 are conducting. Currents *iLk*1 and *iD*1 are continually reduced because leakage energy flowing through diode *D*1 charging capacitor *C*1. The *Lm* is delivering its energy through *T*1 and *D*2 to charge capacitor*C*2 .The energy stored in capacitor *C*3 is constantly delivered to the load. These energy transfers result in falling in *iLk*1 and *iLm* but rising in *iLk* 2 and this mode ends when current *iLk*1 reaches zero at $t = t3$.
4) *Mode IV [t3, t4]:* In this interval, only magnetizing inductor *Lm* is continuously releasing its energy to *C*2. The current pathway is shown in Fig. 4(d), and diode*D*2 is conducting. The *iLm* is reduced due to the magnetizing inductor energy flowing to the coupled inductor *T*1 to secondary winding *N*2, and *D*2 continually to charge capacitor *C*2. The energy stored in capacitor *C*3 is constantly discharged to the load and mode ends when current *iLm* reaches zero at $t = t4$.
5) *Mode V [t4, t5]:* In this interval, active components are turned OFF; the energy stored in capacitor *C*3 is sustained to be discharged to the load. The current pathway is shown in Fig. 4(e) and mode ends when switch *S*1 is turned ON at the start of the next switching period.

III. OPERATION OF THE PROPOSAL METHOD

Nowadays as the technology improved, the steering which is hydraulic previously was changed to electric power steering. Previously the motor used for electric power steering is dc servo motor. Because of the advantages of the BLDC motor, it is used in the electric power steering. BLDC motor consists of stator and rotor. Stator is having a 3 phase winding housed in the slots. Rotor is made up of the permanent magnet. The permanent magnet motors are classified as PM Synchronous motor and PM Brushless DC Motor depending on the back emf s produced. If the back emf produced is sinusoidal then it is called as PM Synchronous motor and if the back emf is trapezoidal then it is called as PM Brushless DC motor.

The BLDC are typically permanent synchronous motor, they are well driven by dc voltage. They have a commutation that is done mainly by electronics application .Some of the man y advantages of a brushless dc motor over the conventional brushed dc motors are highlighted below :

A. Better speed versus torque characteristics
B. High dynamic response
C. High efficiency
D. Long operating life
E. High speed ranges
F. Low maintenance (in terms of brushes cleaning; which is peculiar to the brushed dc motor).

The circuit diagram of the micro converter fed BLDC motor shown in the figure.7. Without step up transformer improved the output voltage with high efficiency, voltage input of the micro converter is 15volt dc supply and output of the micro converter is

Volume 3 Issue III, March 2015
ISSN: 2321-9653
International Journal for Research in Applied Science & Engineering Technology (IJRASET)

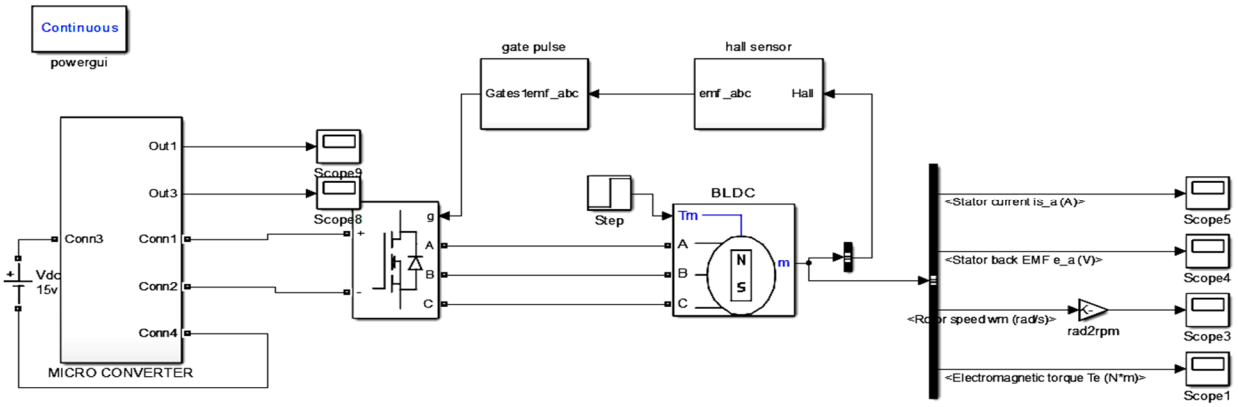

Figure.7.circuit diagram of the micro converter fed BLDC motor

300 volt dc supply and 0.8 amps. Convert the dc supply in ac supply by using the universal bridge is shown in the circuit. Triggering pulse for the power switches generated by pulse generator based on the movement of the motor shaft.

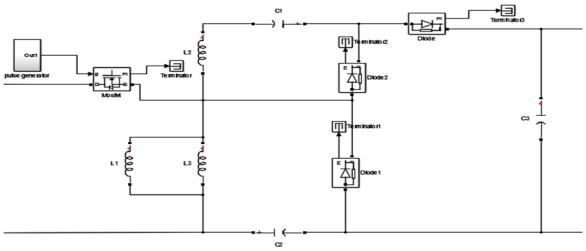

Figure.8. Circuit diagram of the micro converter

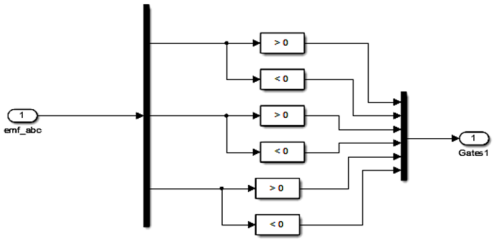

Figure.9.circuit diagram of the pulse generator

In the micro converter only one controlled power electronic switch two uncontrolled power electronic, three inductors and three capacitors are shown in figure .8. The controlled power electronic switch worked based on the triggering pulse, generated by the pulse generator. Figure.9. shown circuit diagram of the pulse generator input of the pulse generator is emf _abc and output of the circuit is trigging pulse to the universal bridge turn on and turn off. Based on the truth table design it generates pulse it shown table.1.

Table.1. Electronic Commutate Output Based on Hall Sensor Signals truth table.

Emf-a	Emf-b	Emf-c	Q1	Q2	Q3	Q4	Q5	Q6
0	0	0	0	0	0	0	0	0
0	-1	+1	0	0	0	1	1	0
-1	+1	0	0	1	1	0	0	0
-1	0	+1	0	1	0	0	1	0
+1	0	-1	1	0	0	0	0	1
+1	-1	0	1	0	0	1	0	0
0	+1	-1	0	0	1	0	0	1
0	0	0	0	0	0	0	0	0

Volume 3 Issue III, March 2015
ISSN: 2321-9653
International Journal for Research in Applied Science & Engineering Technology (IJRASET)

Three upper switches of the inverter are turned on sequentially in the middle of the respective positive voltage half-cycles. The lower devices are chopped in sequence for angles in the respective negative voltage half cycles with the help of decoder for controlling the current.

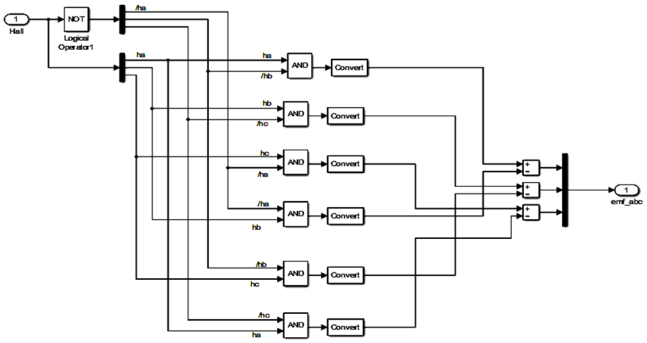

Figure.10.circuit diagram of the Decoder Circuit

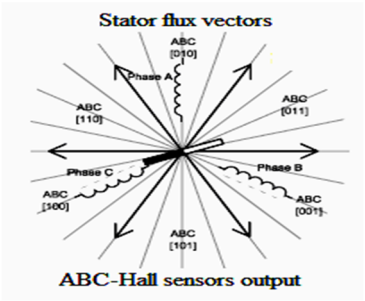

Figure.11 .stator flux vectors

The Hall sensors generate angle phase shifted square waves. These waves are in phase with the respective phase voltage. Each of Hall sensor states correspond to a certain stator flux vector. The Hall sensor states with corresponding stator flux vectors are illustrated in Figure.11. The same information is detailed in Table .1. The decoder circuit is shown in Figure .10. This circuit uses logical AND gates and generates EMFs based on the Hall sensor signals.

Table .2. Truth Table Representation of Stator Vector Flux

ha	hb	hc	Emf_a	Emf_b	Emf_c
0	0	0	0	0	0
0	0	1	0	-1	+1
0	1	0	-1	+1	0
0	1	1	-1	0	+1
1	0	0	+1	0	-1
1	0	1	+1	-1	0
1	1	0	0	+1	-1
1	1	1	0	0	0

The design of the BLDC motor are shown in the tabulations, they are configuration, parameters and advanced.

Table.3. BLDC motor specifications

Sno	configuration	Types
1	Number of phases	3
2	Back EMF waveform	Trapezoidal
3	Machine input	Torque Tm

Sno	parameters	Values
1	Stator phase resistance Rs (ohm)	2.8750
2	Stator phase inductance Ls (ohm)	8.5e-3
3	Flux linkage established by magnets(V.s)	0.175
4	Voltage constant (v_ peak L-L/ k rpm)	73.3038
5	Torque constant(N.m/A_peak)	0.7
6	Back EMF flat area (degrees)	120
7	Inertia, viscous damping ,pole pairs, static friction[J(kg.m^2) F (N.m.s) p() Tf(N.m)]	0.8e-3,1e3,2
8	Initial conditions [Wm(rad/s) thetam (deg) ia,ib(A)]	0,0,0,0

Sno	Advanced	Types
1	Sample time(-1 for inherited)	-1
2	Rotor flux position when theta=0	90 degrees behind phase A axis (modified park)

BLDC motor specification are shown in the above table output of the universal bridge is fed the BLDC motor and it output waveform are verified by the matlab simulink.

IV. RESULTS AND DISCUSSION

The performance of the BLDC motor are discussed in this division,the the micro converter parameters used in the MATLAB/simunk mode are shown in the below tabulation.

Tabul.4.system parameters.

1	Micro converter input	15V
2	Micro converter output voltage	300V
3	Micro converter output current	0.8A
4	Micro converter capacitor C1,C2,C3	47µF,47µF,220µF
5	Micro converter inductance L1,L2,Lm	24.785mH,1.547mH,1.547mH

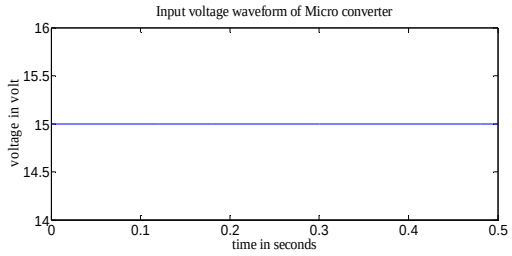

Figure.12.Input voltage waveform of the micro converter

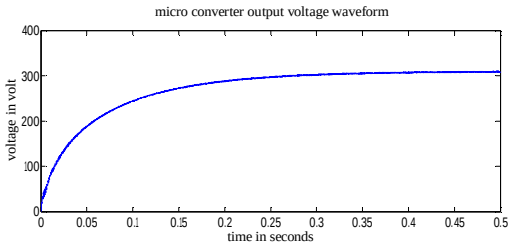

Figure.13.Output voltage waveform of the micro converter

Volume 3 Issue III, March 2015
ISSN: 2321-9653
International Journal for Research in Applied Science & Engineering Technology (IJRASET)

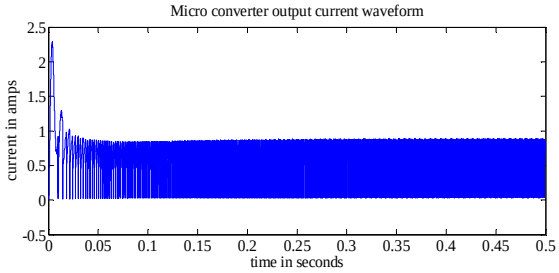

Figure.14.Output current waveform of the micro converter

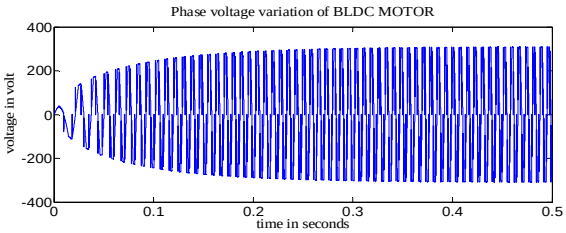

Figure.15.Phase voltage variation of BLDC motor

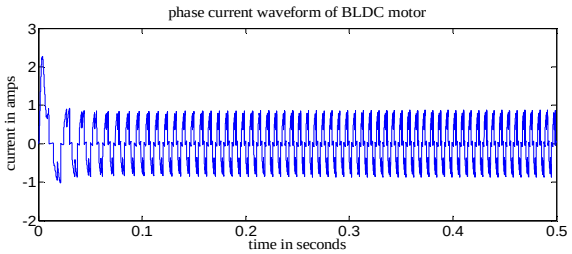

Figure.16.Phase current waveform of BLDC motor

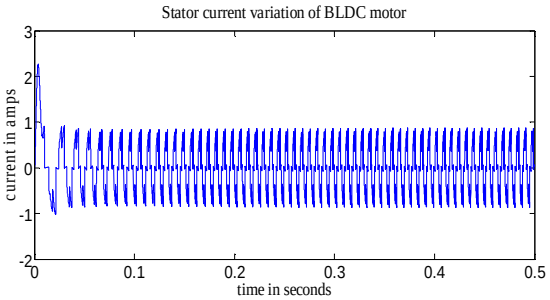

Figure .17.Speed variation waveform of BLDC motor

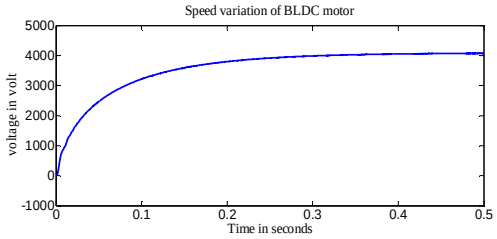

Figure.18.Stator current variation of BLDC motor

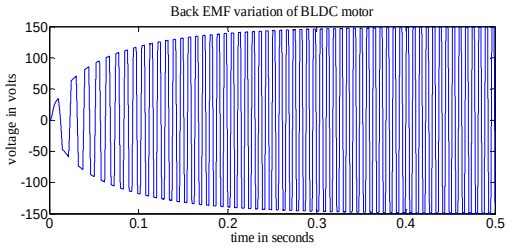

Figure.19.Backemf variation of BLDC motor

The performance of the BLDC motor is shown in above waveforms. input voltage waveform of micro converter, output voltage waveform, output current waveform, phase voltage variation of BLDC motor, .phase current waveform of BLDC motor, speed variation waveform of BLDC motor, stator current variation of BLDC motor and back emf variation of BLDC motor waveforms are shown in above figures, waveform analysis for the simulation period is 0.5 seconds. Input of the micro converter is 15volt dc supply step up into 300 volts dc and 0.8 amps. Phase voltage variation of the BLDC motor is 300 volt ac supply and current waveform of the BLDC motor is 0.8 ac supply. Speed of the BLDC motor is 4000 rpm at no load condition.

V. CONCLUSION

Since the energy of the coupled inductor's leakage inductor has been reused, the voltage stress across the switch *S*1 is constrained, which means low ON-state resistance can be selected. Improvements to the efficiency of the converter have been achieved and fed the output to the BLDC motor input. The switching signal action is performed well by the balanced switch during system operation; on the other hand, the energy is effectively eliminated during the non operating condition, which improves protection to system

technicians. From this prototype converter, the turns ratio n = 5 and the duty ratio D is 55%; thus, without extreme duty ratios and turns ratios, the proposed converter step-up voltage gain, of up to 20 times the level of input voltage. The results show that the maximum efficiency. The performance of the BLDC motor also very efficiency verified by the matlab simulink.

REFERENCES

[1] T. Shimizu,K.Wada, andN.Nakamura, "Flyback-type single-phase utility interactive inverter with power pulsation decoupling on the dc input for an ac photovoltaic module system," *IEEE Trans. Power Electron.*, vol. 21, no. 5, pp. 1264–1272, Jan. 2006.
[2] C. Rodriguez and G. A. J. Amaratunga, "Long-lifetime power inverter for photovoltaic ac modules," *IEEE Trans. Ind. Electron.*, vol. 55, no. 7, pp. 2593–2601, Jul. 2008.
[3] S. B. Kjaer, J. K. Pedersen, and F. Blaabjerg, "A review of single-phase grid-connected inverters for photovoltaic modules," *IEEE Trans. Ind. Appl.*, vol. 41, no. 5, pp. 1292–1306, Sep./Oct. 2005.
[4] J. J. Bzura, "The ac module: An overview and update on self-contained modular PV systems," in *Proc. IEEE Power Eng. Soc. Gen. Meeting*, Jul. 2010, pp. 1–3.
[5] B. Jablonska, A. L. Kooijman-van Dijk, H. F. Kaan, M. van Leeuwen, G. T. M. de Boer, and H. H. C. de Moor, "PV-PRIV´E project at ECN, five years of experience with small-scale ac module PV systems," in *Proc. 20th Eur. Photovoltaic Solar Energy Conf.*, Barcelona, Spain, Jun. 2005, pp. 2728–2731.
[6] T. Umeno, K. Takahashi, F. Ueno, T. Inoue, and I. Oota, "A new approach to lowripple-noise switching converters on the basis of switched- capacitor converters," in *Proc. IEEE Int. Symp. Circuits Syst.*, Jun. 1991, pp. 1077– 1080.
[7] B. Axelrod, Y. Berkovich, and A. Ioinovici, "Switched-capacitor/ switched-inductor structures for getting transformerless hybrid dc–dc PWM converters," *IEEE Trans. Circuits Syst. I, Reg. Papers*, vol. 55, no. 2, pp. 687–696, Mar. 2008.
[8] B. Axelrod, Y. Berkovich, and A. Ioinovici, "Transformerless dc–dc converters with a very high dc line-to-load voltage ratio," in *Proc. IEEE Int. Symp. Circuits Syst. (ISCAS)*, 2003, vol. 3, pp. 435–438.
[9] H. Chung and Y. K. Mok, "Development of a switched-capacitor dc–dc boost converter with continuous input current waveform," *IEEE Trans. Circuits Syst. I, Fundam. Theory Appl.*, vol. 46, no. 6, pp. 756–759, Jun 1999.
[10] T. J. Liang and K. C. Tseng, "Analysis of integrated boost-flyback step-up converter," *IEE Proc. Electrical Power Appl.*, vol. 152, no. 2, pp. 217–225, Mar. 2005.
[11] Q. Zhao and F. C. Lee, "High-efficiency, high step-up dc–dc converters," *IEEE Trans. Power Electron.*, vol. 18, no. 1, pp. 65–73, Jan. 2003.
[12] M. Zhu and F. L. Luo, "Voltage-lift-type cuk converters: Topology and analysis," *IET Power Electron.*, vol. 2, no. 2, pp. 178–191, Mar.2009.
[13] J. W. Baek, M. H. Ryoo, T. J. Kim, D. W. Yoo, and J. S. Kim, "High boost converter using voltage multiplier," in *Proc. IEEE Ind. Electron. Soc. Conf. (IECON)*, 2005, pp. 567–572.
[14] J. Xu, "Modeling and analysis of switching dc–dc converter with coupledinductor," in *Proc. IEEE 1991 Int. Conf. Circuits Syst. (CICCAS)*, 1991, pp. 717–720.
[15] R. J.Wai, C. Y. Lin, R. Y. Duan, and Y. R. Chang, "High-efficiency dc–dc converter with high voltage gain and reduced switch stress," *IEEE Trans. Ind. Electron.*, vol. 54, no. 1, pp. 354–364, Feb. 2007.
[16] S. H. Park, S. R. Park, J. S. Yu, Y. C. Jung, and C. Y. Won, "Analysis and design of a soft-switching boost converter with an HI-Bridge auxiliary resonant circuit," *IEEE Trans. Power Electron.*, vol. 25, no. 8, pp. 2142– 2149, Aug. 2010.
[17] H. Mao, O. Abdel Rahman, and I. Batarseh, "Zero-voltage-switching dc–dc converters with synchronous rectifiers," *IEEE Trans. Power Electronics.*,vol. 23, no. 1, pp. 369–378, Jan. 2008.
[18] [25] J. M. Kwon and B. H. Kwon, "High step-up active-clamp converter wit input-current doubler and output-voltage doubler for fuel cell power systems," *IEEE Trans. Power Electron.*, vol. 24, no. 1, p. 108–115, Jan. 2009.

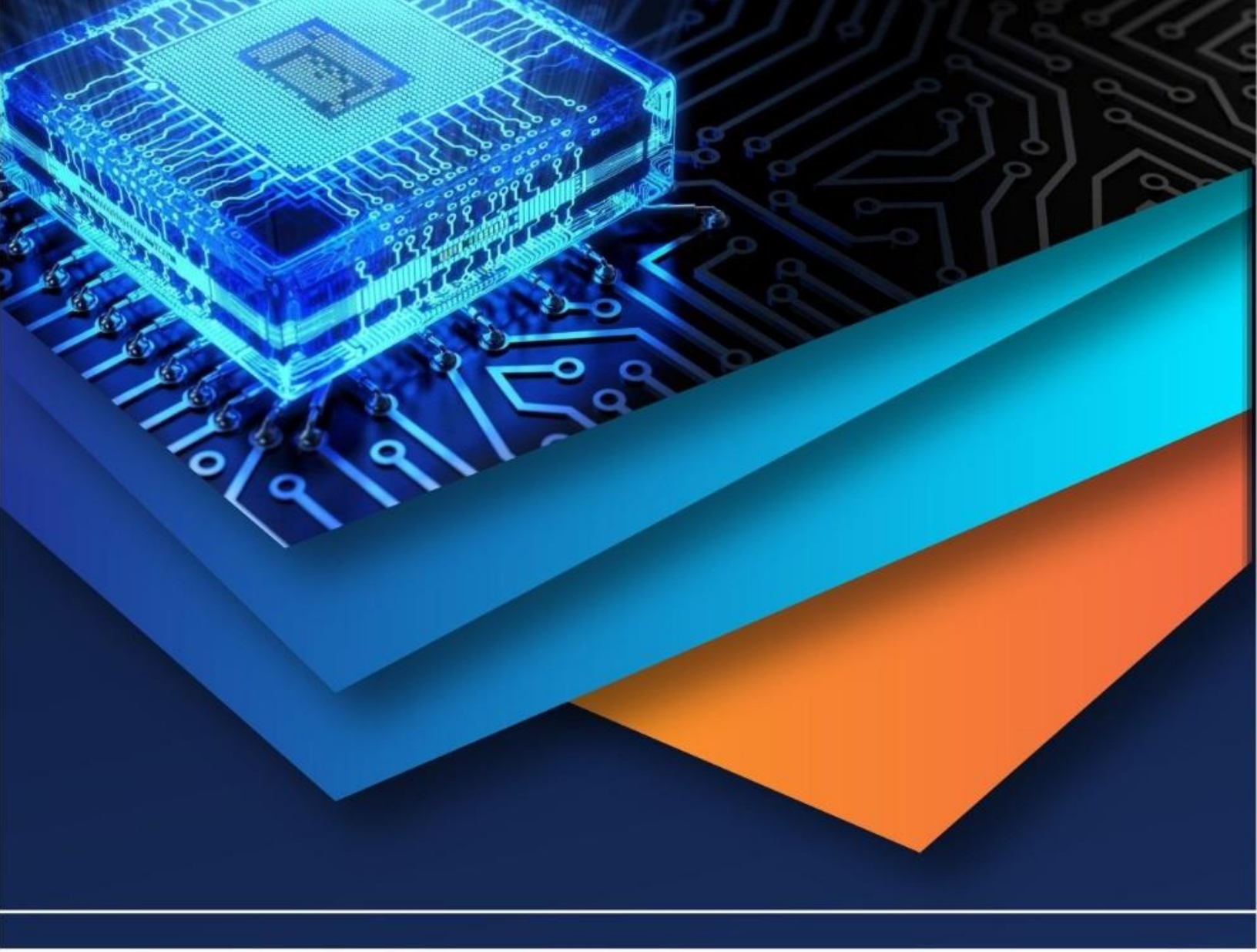

10.22214/IJRASET

45.98

IMPACT FACTOR: 7.129

IMPACT FACTOR: 7.429

INTERNATIONAL JOURNAL FOR RESEARCH

IN APPLIED SCIENCE & ENGINEERING TECHNOLOGY